

# GaN Heterostructure Barrier Diodes (HBD) with Polarization-Induced Delta-Doping

Pei Zhao\*, Amit Verma, Jai Verma, Huili Xing, Patrick Fay and Debdeep Jena

Department of Electrical Engineering, University of Notre Dame, Notre Dame, IN 46556, USA

Phone: (574)631-1290 Email: \*pzhao@nd.edu

**Background:** The nonlinear characteristics of solid-state devices are widely used for high frequency applications such as mixers, detectors, and frequency multipliers; for example, the nonlinear rectifying behaviors of Schottky and heterostructure backward diodes are widely used for mixing and detection. Improved flexibility in device design while retaining a rectifying  $I$ - $V$  can be realized by back-to-back Schottky diodes, such as by p-type  $\delta$ -doping in the middle of an intrinsic GaAs layer, known as the Planar Doped Barrier (PDB) diode (Figure 1) [1]. The barrier height and depletion region thickness  $L_1$  and  $L_2$  are decided by the position and concentration of the  $\delta$ -doping (Figure 1 (d)). A reliable PDB is limited by the control of  $\delta$ -doping. In III-Nitride heterostructures, due to the presence of a high spontaneous and piezoelectric polarization charge, an effective  $\delta$ -doping can be induced at sharp heterojunctions with atomic control and doping densities far beyond what is achievable by chemical acceptor (or donor)  $\delta$ -doping in other III-V semiconductors. Polarization-induced sheet charges have not yet been exploited for HBD design in the III-Nitride system; this work presents preliminary results in that direction.

**Device structure design:** The designed GaN Heterostructure Barrier Diode shown in Figure 2 is grown by plasma-assisted molecular beam epitaxy (MBE). The substrate is Ga - face  $n^+$  bulk GaN from Ammono with dislocation density less than  $10^5$   $\text{cm}^{-2}$  [2]. A 24nm thick region graded from GaN  $\rightarrow$   $\text{Al}_{0.75}\text{Ga}_{0.25}\text{N}$  is following a 20nm thick unintentional doped (UID) GaN. This region is surrounded by heavily n-type doped GaN contact regions. In the linearly graded AlGaIn, polarization induces a bulk (3D) charge (Figure 2 (b)), and at the abrupt  $\text{Al}_{0.75}\text{Ga}_{0.25}\text{N}/\text{GaN}$  junction, a  $\delta$ -doping sheet similar to a PDB is formed naturally without chemical doping. A barrier is thus formed as shown (Figure 2 (d)). At high Al composition, the negative polarization sheet charge is so high that a 2D hole gas (2DHG) can be induced at the interface. An n-type  $\delta$ -doping at the interface could compensate the hole gas (Figure 3 (a)). In this work, we fix the Al composition and compare the  $CV$  and  $IV$  with and without  $\delta$ -doping. Three different HBD structures are shown here: a) HBD-A (24nm graded region, 20nm UID-GaN); b) HBD-B (24nm graded region, 20nm UID-GaN, 4nm  $\delta$ -doping at interface); and c) HBD-C (24nm graded region, 45nm UID-GaN).

**Results and discussions:** Figure 3 (a) shows the energy band diagrams of HBD-A and HBD-B at  $V = 1\text{V}$ . Because the depletion region thickness does not vary appreciably with bias (same for PDB), the capacitance is flat and is precisely the parallel-plate capacitance of the depleted GaN (Figure 3(b)). The  $\delta$ -doping is near the interface, which has a small influence on the depletion thickness and capacitance. The capacitance of HBD-C with 45nm UID-GaN is shown as a comparison (bottom solid line). The constant capacitance decreases as the UID-GaN thickness increases. Similar to PDB, the  $IV$  characteristic depends on the ratio of depletion lengths  $L_1/L_2$ . With  $L_1/L_2 = 1$  (HBD-A), a symmetric  $IV$  is observed in Figure 4 (a) and an asymmetric  $IV$  results in HBD-C with  $L_1/L_2 = 0.4$  (Figure 4 (b)). The calculated  $IV$  curve is based on a simple thermionic emission model of PDBs [3], and it roughly captures the experimental data (Figure 4 and Figure 5). We note that in the thermionic emission model, carriers contributing to transport are assumed to be thermalized (near the conduction band edge). Due to the large band offset at the AlGaIn/GaN interface, hot electrons possibly play a role and must be considered in future work. Figure 6 shows the  $IV$  characteristics comparison between all three HBDs. A lower current density is observed in HBD-B (with  $\delta$ -doping) compared with HBD-A. The reason for this observation is still under investigation. GaN HBDs could be used as mixers, and detectors as has been demonstrated for PDB diodes [4-5]. The  $IV$  characteristics and the corresponding curvature coefficient are shown in Figure 7. The zero bias curvature is  $\sim 8/V$  and the peak curvature is about  $10 \sim 30/V$ . The curvature coefficient is less than the ideal Schottky curvature coefficient  $q/k_B T \sim 38/V$ . Although more understanding is required, GaN HBD can offer the same circuit possibilities as PDB. In addition to the doping induced thermionic barrier, barriers can also be induced by the band offsets at heterostructure interfaces such as GaAs/AlGaAs/GaAs. This type of a device is called the Heterostructure Barrier Varactor (HBV) diode, which offers higher efficiency for frequency multiplication [6]. For high-frequency applications, GaN HEMTs are approaching  $\sim 0.5$  THz cutoff frequencies [7], and  $\sim 0.3$  THz HEMT-based RF power sources are in the horizon. GaN HBDs or varactor using atomically sharp polarization-induced planar doping can be directly integrated with nitride HEMTs, and serve as frequency multipliers. Some advantages may include the high thermal conductivity, high breakdown, extremely low contact resistance, polarization-induced atomically sharp charges and the corresponding scaling capability in the III-Nitride system. In addition, due to the large band offset at the AlGaIn/GaN interface, GaN HBD can also take advantage of hot-electron injection. The kinetic energy of the injected electrons can be higher than the inflection point in the conduction band where the negative effective mass (NEM) exists [8]. NEM based oscillator and amplifiers has been proposed back in 1950s [9-10]. Such hot-carrier transport phenomena and negative-effective mass oscillators (NEMO) can potentially enable 2-terminal high-frequency oscillators as an extension of the HBD itself. This work presents a step in that direction. (This work is funded by the Office of Naval research (Dr. Paul Maki) [DATE MURI].)

**References:** [1] R.J. Malik, et al. Elec. Lett. 16, 836, 1980. [2] AMMONO, www.ammono.com [3] S. M. Sze, "High-speed semiconductor devices." New York, Wiley-Interscience, 1990. [4] M.J. Kearney, et al. Elec. Lett. 27, 721, 1991. [5] S. Dixon Jr, and R. J. Malik. U.S. Patent No. 4,563,773. 1986. [6] E. Kollberg, et al. Elec. Lett. 25, 1696, 1989. [7] Y. Yue, et al. Elec. Dev. Lett. 33, 988, 2012. [8] A. Dyson and B. K. Ridley. Phys. Rev. B 72, 193301, 2005. [9] H. Kromer, Phys. Rev. 109, 1856, 1958. [10] H. Kromer, Proceedings of the IRE 47, 397, 1959

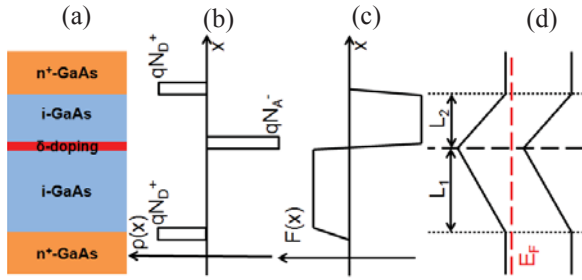


Figure 1 (a) Structure of GaAs planar doped barrier diode, (b) charge distribution, (c) electric field distribution, and (d) energy band diagram at zero bias.

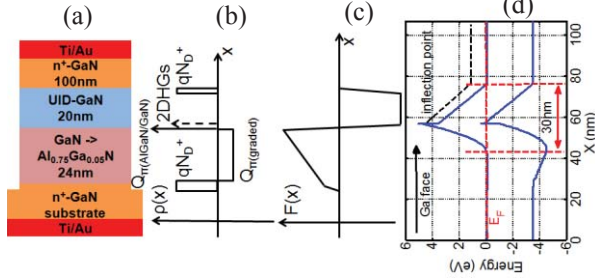


Figure 2 (a) Structure of GaN heterostructure barrier diode with contact metals, (b) charge distribution with bulk polarization charge in the graded region, polarization sheet at AlGaIn/GaN interface and 2DHG, (c) electric field distribution, and (d) energy band diagram of the active region and the contact layers at zero bias.

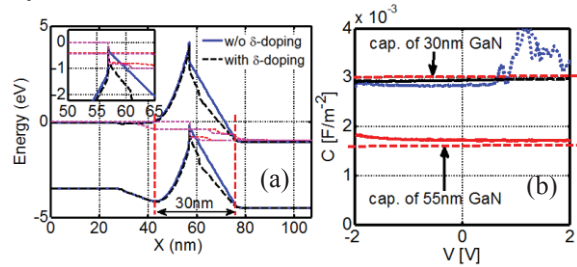


Figure 3 (a) Band diagrams of GaN HBD (20nm UID-GaN) at  $V = 1V$ .  $\delta$ -doping compensates the 2DHG (dashed lines). (b) CV comparison of HBD-A (dotted line) and HBD-B (top solid line). The bottom solid line is capacitance of HBD-C.

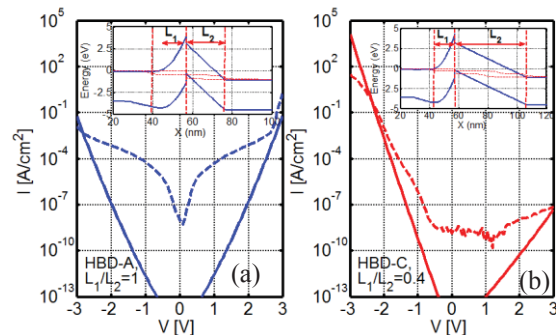


Figure 4 Comparison of the measured (dashed lines) and the calculated (solid lines)  $IV$  characteristics of

HBD with current density in log scale (a)  $L_1/L_2=1$  and (b)  $L_1/L_2=0.4$ .

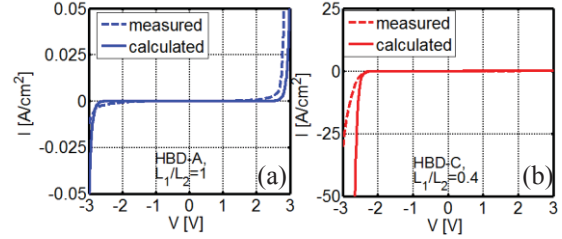


Figure 5 Comparison of the measured and the calculated  $IV$  characteristics of HBD with current density in linear scale (a) symmetric  $IV$  with  $L_1/L_2=1$  and (b) backward diode behavior at  $L_1/L_2=0.4$ .

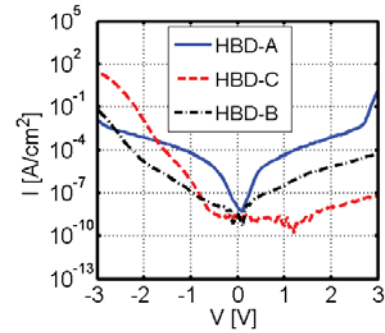


Figure 6  $IV$  comparisons between all three HBDs.

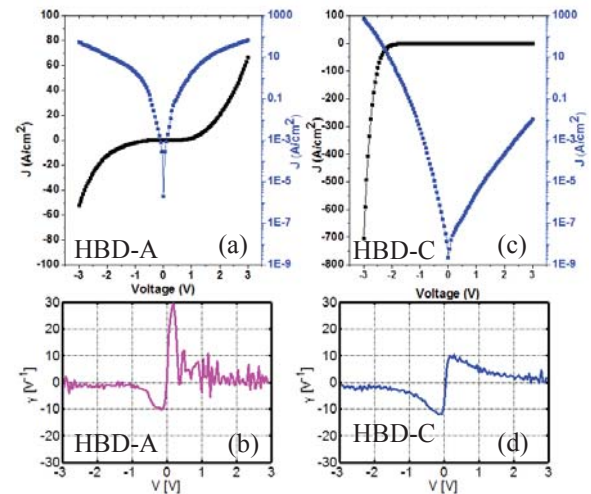


Figure 7  $IV$  characteristics and corresponding curvature coefficient for HBD-A ((a) and (b)) and HBD-C ((c) and (d)).